Bound States of ^{3}He at the Edge of a ^{4}He Drop on a Cesium Surface

R. Mayol,[1] M. Barranco,[1] E. S. Hernández,[2] M. Pi,[1] and M. Guilleumas[1]

[1]*Departament ECM, Facultat de Física, Universitat de Barcelona, E-08028 Barcelona, Spain*

[2]*Departamento de Física, Facultad de Ciencias Exactas y Naturales, Universidad de Buenos Aires, 1428 Buenos Aires, Argentina*

(Received 8 October 2002; published 8 May 2003)

We show that small amounts of ^{3}He atoms, added to a ^{4}He drop deposited on a flat cesium surface at zero temperature, populate bound states localized at the contact line. These edge states show up for drops large enough to develop well defined surface and bulk regions together with a contact line, and they are structurally different from the well-known Andreev states that appear at the free surface and at the liquid-solid interface of films. We illustrate the one-body density of ^{3}He in a drop with 1000 ^{4}He atoms, and show that for a sufficiently large number of impurities the density profiles spread beyond the edge, coating both the curved drop surface and its flat base and eventually isolating it from the substrate.

DOI: 10.1103/PhysRevLett.90.185301 PACS numbers: 67.60.–g, 61.46.+w, 67.70.+n

During the last decade, experimental and theoretical studies of wetting phenomena on substrates of various adsorptive strengths have considerably enriched the physics of quantum fluids. Liquid ^{4}He, which was early believed to be a universal wetting agent, exhibits finite wetting temperatures on cesium surfaces [1]. On the other hand, the theoretical prediction that ^{3}He is a universal wetting agent [2] was confirmed by measurements of its adsorption isotherms on Cs [3]. These opposite and complementary wetting properties combine in a very interesting manner when the helium isotopes coexist in a low-temperature solution, since ^{3}He dissolved into bulk liquid or ^{4}He films populate a two-dimensional homogeneous layer of Andreev states on the free surface (see, e.g., Ref. [4] and references therein).

Andreev-like states for a single ^{3}He atom, localized at the liquid-substrate interface of a ^{4}He film on a variety of adsorbers, including weak alkalis like Cs, were predicted within the frame of density functional (DF) theory [5]. The effect of ^{3}He impurities on the liquid-vapor and liquid-solid surface tensions of ^{4}He on Cs is a key ingredient in the prediction of reentrant wetting by helium mixtures [6], as measured shortly afterwards [7,8]. The existence of the interfacial bound states was confirmed by experimental evidence [9] and by microscopic variational calculations [10]. More recent measurements of the contact angle of helium mixtures on Cs [11] showed that the large observed values are consistent with both single-particle (sp) states of the ^{3}He atoms at the liquid-solid interface and surface excitations.

The preference of ^{3}He to migrate to the surface of ^{4}He is a very general consequence of the mutual interaction between the isotopes, and this structure appears as well in density profiles of mixed drops as described by DF theory [12–14]. These descriptions of finite helium mixtures consider freely standing systems in vacuum; however, mixed clusters deposited on adsorbing substrates offer an interesting illustration of the competition between self-saturation, mutual interaction between the helium isotopes and external confinement, with consequences on their wetting behavior. A theoretical approach has been anticipated for droplets of pure ^{4}He on Cs, whose profiles and contact angles have been recently computed [15], employing a finite range density functional (FRDF) [16] at zero temperature.

In this Letter, we present DF calculations of nanoscale mixed ^{3}He-^{4}He droplets at zero temperature on a flat Cs surface using the FRDF for mixtures of Ref. [17] and demonstrate that the lowest-lying ^{3}He sp bound states are localized on the perimeter of the ^{4}He base, i.e., the contact line. These are genuine edge states of a different nature than the well-known Andreev ones, since they originate in the peculiarities of the mean field for this specific geometry.

For this sake, assuming axial symmetry around the z axis perpendicular to the Cs substrate, by functional differentiation of the energy density we derive the Euler-Lagrange (EL) equation for the ^{4}He particle density $\rho_4(r, z)$ and the Kohn-Sham (KS) equations for the ^{3}He sp wave functions (wf's) $\psi_{nl}(r, z)\, e^{il\varphi}$, with l the z projection of the orbital angular momentum, for fixed particle numbers N_i ($i = 3, 4$). The general form of these equations can be found in Ref. [13]; hereafter we shall mostly restrict our considerations to the case $N_4 = 1000$ and varying N_3 as discussed below.

The first problem that we solve is the Schrödinger equation for one ^{3}He atom in the field of a ^{4}He cluster on a Cs surface, with the Cs-He potential of Ref. [15]. In Fig. 1 we show contour plots on the $y = 0$ plane (hereafter, lengths are given in Å) of the probability densities $|\psi_{n0}(r, z)|^2$ for $n = 1$, 2, and 3, together with gray-scale views of the density $\rho_4(r, z)$, which exhibits the layered structure encountered in films on flat surfaces [18] (see also Ref. [15]).

The most spectacular result is undoubtedly the appearance of the $1s$ ground state (gs) ψ_{10}, since the sharp localization of the impurity on the contact line indicates the existence of a new kind of sp state, the edge state. With

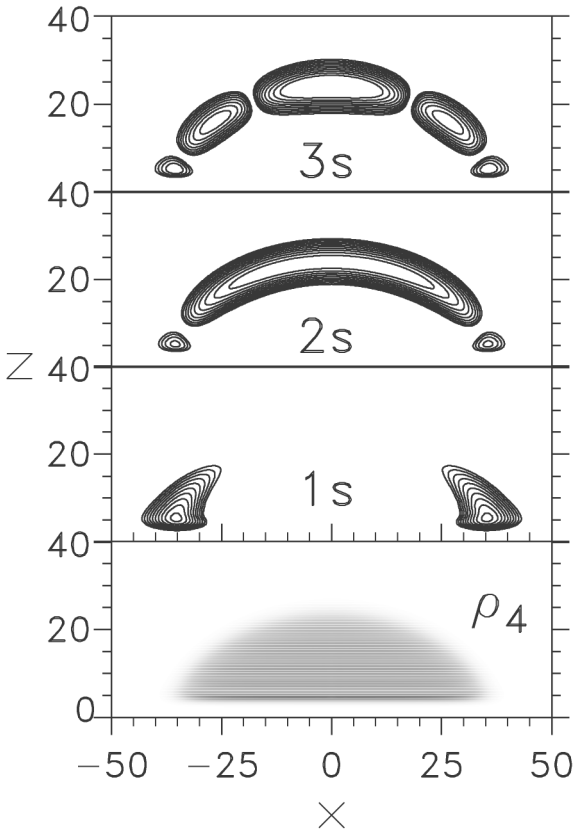

FIG. 1. Probability densities of s states of a ^{3}He atom together with the ^{4}He particle density in the $y = 0$ plane for a drop with $N_4 = 1000$.

a truly one-dimensional (1D) probability density on a ring of mesoscopic size, it would certainly exist in a macroscopic droplet, being in essence a 1D analog of the two-dimensional Andreev state at the planar free surface of ^{4}He. Its origin is the density distribution of the ^{4}He drop that, together with the potential created by the substrate, gives rise to the strong attraction experienced by the impurity near the contact line. In addition, the enhanced surface width of the ^{4}He cluster at the edge, due to the overlapping spreads of both the upper and the lower surfaces, permits large zero point motion of the impurity, thus lowering its kinetic energy and favoring binding.

We display in Fig. 2 the evolution of the sp energy ε_{1s} with N_4, which shows that for relatively small sizes (around $N_4 = 2000$), the curve seems to be asymptotic to a certain value, the macroscopic limit. We have verified as well that s states with n between 2 and 8 span an energy shell, with a width of about 1.3 K starting at $\varepsilon_{20} = -4.74$ K, for, i.e., $N_4 = 1000$ (cf. Fig. 3), that could be regarded as fragmentation of the Andreev state of the free surface of films, induced by finite size and curved shape. This is supported by the shape of the excited probability densities displayed in Fig. 1, which display peaks on the upper surface of the drop.

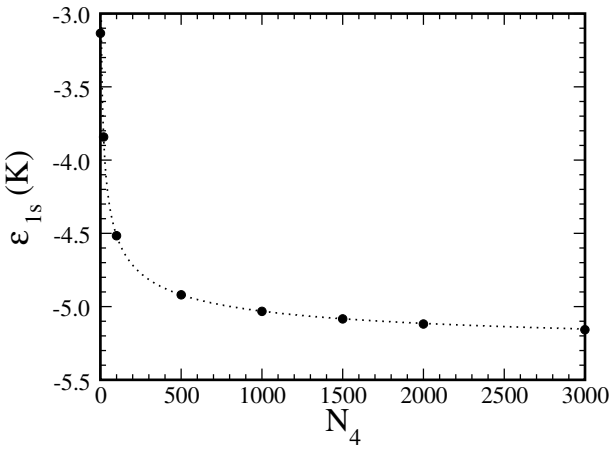

FIG. 2. Energy of the 1s state for $N_4 = 20$, 100, 500, 1000, 1500, 2000, and 3000. The calculated energy of one single ^{3}He atom on a Cs substrate is also given. The dotted line has been drawn as a guide to the eye.

Noticeably also, we have found that the probability densities $|\psi_{1l}(r, z)|^2$ for $l > 0$ are essentially identical to $|\psi_{10}(r, z)|^2$. This reflects the fact that these excitations consist of rotations of the gs ψ_{10} around the symmetry axis of the ^{4}He drop, as can be seen in the sp level scheme depicted in Fig. 3. Instead, since s-excited states possess nonvanishing probability density on the rotational axis, states with $n > 1$ and $l > 0$ are more sensitive to the centrifugal potential that splits the cusp creating extra lobes in the higher levels described by wf's $\psi_{nl}(r, z)$.

For the rotational band, the sp energies follow the rule

$$\varepsilon_{1l} = \varepsilon_{10} + \frac{\hbar^2 l^2}{2m^*_{10}R^2_{10}} \tag{1}$$

with $\varepsilon_{10} = -5.03$ K. Effective masses m^*_{nl}, defined as the state averages of the local, density-dependent one [5],

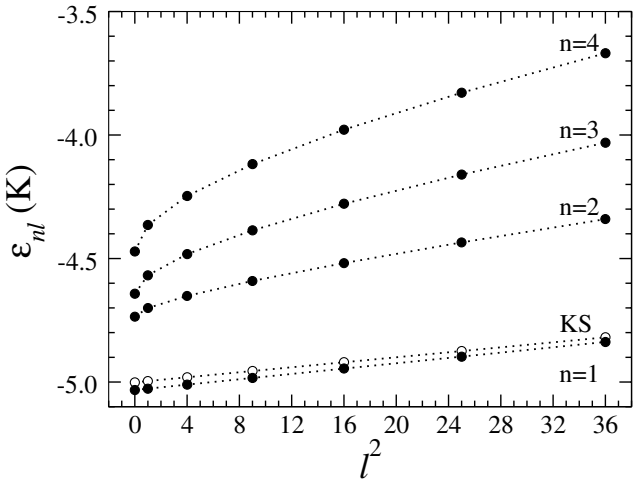

FIG. 3. Spectrum of a single ^{3}He atom as a function of squared angular momentum for the bands $n = 1$ to 4, together with the KS energies of the occupied sp levels corresponding to $N_3 = 26$ (open circles), with dotted lines to guide the eye.

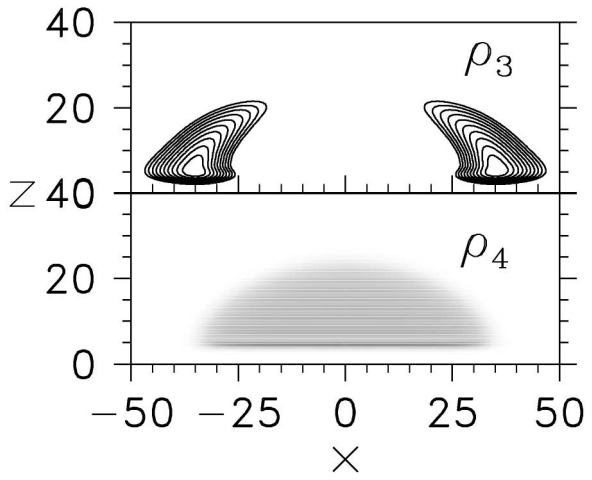

FIG. 4. The EL/KS ^{3}He and ^{4}He particle densities for $N_3 = 26$ and $N_4 = 1000$.

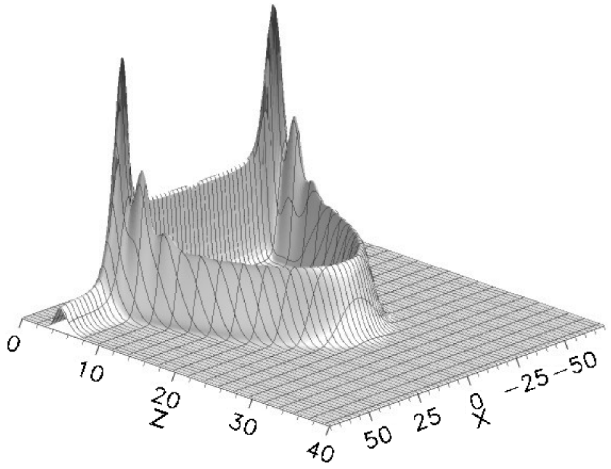

FIG. 5. Three-dimensional view of the ^{3}He particle density in the $y = 0$ plane for $N_4 = 1000$ and $n_3 = 3 \times 10^{-3}$ Å^{-2}. The highest density peaks correspond to $\rho_3 \sim 1.4 \times 10^{-2}$ Å^{-3}.

$$\frac{1}{m^*_{nl}} = \int d\vec{r} \frac{1}{m^*_3[\rho_4(r,z)]} [\psi_{nl}(r,z)]^2, \qquad (2)$$

are parameters that appear naturally in the prefactor of the centrifugal potential as one computes the expectation value of the sp Hamiltonian. In this case, we obtain $m^*_{10} = 1.21 m_3$, which together with the slope of the linear regression in Fig. 3 gives a gs radius $R_{10} = 35.1$ Å. We point out that if $m^*_{10} = m_3$, the corresponding values $\varepsilon_{10} = -4.86$ K and $R_{10} = 34.7$ Å reveal the scarce relevance of this parameter to our main results. For the s states $n = 2$ to 8, the respective m^*_{n0} are similar and close to $1.3 m_3$, which scales with the effective mass for the Andreev surface state in ^{4}He films on Cs [6,10,19], around $1.45 m_3$.

As a second step, we have solved the system consisting of the coupled EL/KS equations, for N_3 values corresponding to closed shell configurations made of sp states within the gs rotational band. For small N_3 values, the level filling sequence still corresponds to the sp spectrum of a single atom, with slightly decreasing slopes of the gs rotational band, due to the finite ^{3}He density which enhances the effective mass, and smaller values of $|\varepsilon_{10}|$ also depending on N_3. This is illustrated in Fig. 3 for $N_3 = 26$. The shape of the wf's $\psi_{1l}(r, z)$ below the Fermi sea is now sensitive to N_3, and $\rho_4(r, z)$ is also affected; maps of the ^{3}He and ^{4}He particle densities, with details as in Fig. 1, are depicted in Fig. 4, showing the tendency of the ^{3}He density to drift upwards on the drop surface; note that the lowest ^{3}He density line corresponds to 10^{-6} Å^{-3}.

A substantial simplification of the above full coupled problem, within excellent accuracy for sufficiently large N_3, is provided by the Thomas-Fermi method [20]. We apply this procedure to $N_3 \geq 100$, and find that at $N_3 = 100$, the density profile of the impurities covers the free surface of the ^{4}He drop, and tends to isolate it from the substrate. For N_3 between 100 and 150, the situation qualitatively changes, and ^{3}He spreads beyond the edge of the ^{4}He drop giving rise to a thin film of ^{3}He that coats the Cs substrate with an asymptotic coverage n_3. As our interest here is in finite systems, we have just solved the problem of the splashed ^{4}He$_{1000}$ droplet for two very low asymptotic coverages, namely, $n_3 = 2 \times 10^{-3}$ and 3×10^{-3} Å^{-2}.

Figure 5 is a three-dimensional view of $\rho_3(r, z)$ corresponding to $n_3 = 3 \times 10^{-3}$ Å^{-2}, where the occupied edge states of the single atoms can be visualized as large peaks near the contact line, while Fig. 6 exhibits the corresponding $\rho_4(r, z)$. The layering of the ^{3}He density appears as a series of peaks on the covering shell on the ^{4}He cluster; in addition, we note the spreading of $\rho_3(r, z)$ near the substrate as r increases beyond the region populated by the edge states. In this case, the number of ^{3}He atoms inside a cylinder of radius $R = 50$ Å is ~180, and ~138 for $n_3 = 2 \times 10^{-3}$ Å^{-2}.

Finally, we comment on the contact angle, whose determination for nanoscopic droplets is far from trivial, as

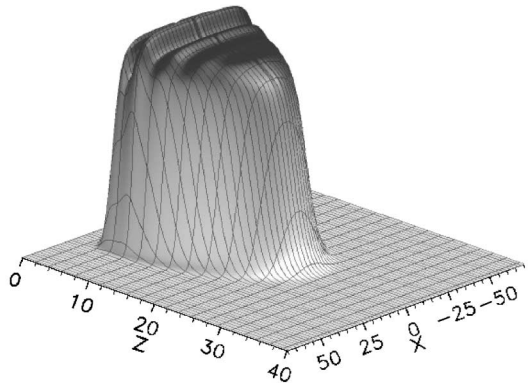

FIG. 6. Three-dimensional view of the ^{4}He particle density in the $y = 0$ plane for $N_4 = 1000$ and $n_3 = 3 \times 10^{-3}$ Å^{-2}. The highest density ridge corresponds to $\rho_4 \sim 2.4 \times 10^{-2}$ Å^{-3}.

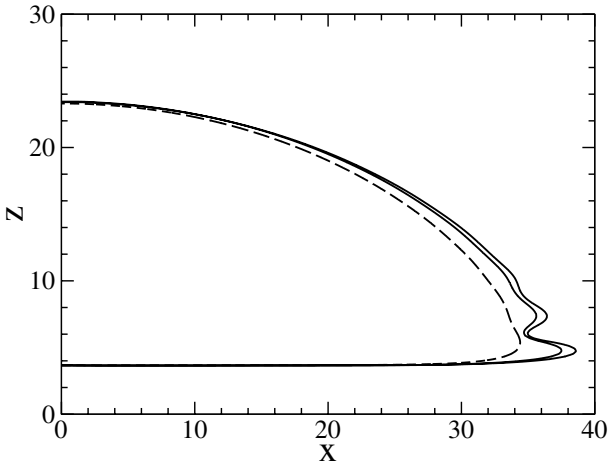

FIG. 7. Contour plots of the total ^{3}He + ^{4}He density corresponding to 0.011 Å^{-3} for the case $N_4 = 1000$ and $n_3 = 2 \times 10^{-3}$ Å^{-2}, $n_3 = 3 \times 10^{-3}$ Å^{-2}. The dashed line corresponds to the pure ^{4}He drop.

discussed in [15]. We have seen that helium droplet densities display non-negligible surface widths and are highly stratified near the substrate. This structure renders the contact angle an ill defined quantity, and one has to resort to methods such as that in [15], since a determination of the contact angle by "visual inspection" of the equidensity lines may lead to only a rather crude estimate. For the pure ^{4}He droplets our results coincide with those of [15], thus the procedure there described would give a contact angle of about 30°.

The presence of ^{3}He affects the contact angle, as can be judged from Fig. 7, where we show the contour plot of the total ^{3}He + ^{4}He density corresponding to roughly half the bulk ^{4}He density for $N_4 = 1000$ and the above two ^{3}He coverages. It appears from this figure that whereas the height of the cap does not change visibly, the radius of the cap base increases by 8%–10%, and this should have a sizable effect in any sensible determination of the contact angle.

To summarize, we have found that in addition to the well-known Andreev states, ^{4}He drops on Cs substrates host a new class of ^{3}He sp states which appear as 1D rings of ^{3}He atoms surrounding the contact line for mesoscopic drops or wedges, and are the lowest lying. The gs energies found in this work are, for the largest clusters, close to those of surface [5,19] Andreev states, around −5.1 K depending on the ^{4}He coverage, and below the interfacial [9,19] Andreev states, around −4.3 K. The experimental detection of these edge states might be a challenge, open to seeking thermodynamic evidence through specific heat or magnetic susceptibility measurements below the dewetting line of the low-temperature phase diagram for mixtures [8], or dynamical evidence for undamped 1D spin-density oscillations [21]. The statistical model in Ref. [11] shows that the most likely scenario for measured contact angles and surface tensions must include both Andreev states and ripplons at the substrate-liquid interface; accordingly, it might be interesting to examine the effects of the new edge states — so far overlooked — in this description.

This work has been performed under Grant No. BFM2002-01868 from DGI, and Grants No. 2001SGR-00064 and No. ACI2000-28 from Generalitat of Catalunya. E. S. H. has also been funded by M.E.C.D. (Spain). We are grateful to Francesco Ancilotto, Milton Cole, and Adrian Wyatt for useful discussions, and to Eckhard Krotscheck for helpful advice.

[1] P. J. Nacher and J. Dupont-Roc, Phys. Rev. Lett. **67**, 2966 (1991); P. Taborek and J. Rutledge, Phys. Rev. Lett. **68**, 2184 (1992); S. K. Mukherjee, D. P. Drusit, and M. H. W. Chan, J. Low Temp. Phys. **87**, 113 (1992); K. S. Ketola, S. Wang, and R. B. Hallock, Phys. Rev. Lett. **68**, 201 (1992); J. E. Rutledge and P. Taborek, Phys. Rev. Lett. **69**, 937 (1992); P. Taborek and J. Rutledge, Physica (Amsterdam) **197B**, 283 (1994).
[2] L. Pricaupenko and J. Treiner, Phys. Rev. Lett. **72**, 2215 (1994).
[3] D. Ross, J. A. Phillips, J. E. Rutledge, and P. Taborek, J. Low Temp. Phys. **106**, 81 (1997).
[4] R. B. Hallock, J. Low Temp. Phys. **120**, 441 (2000); P.-C. Ho and R. B. Hallock, J. Low Temp. Phys. **120**, 501 (2000).
[5] N. Pavloff and J. Treiner, J. Low Temp. Phys. **83**, 331 (1991); J. Treiner, J. Low Temp. Phys. **92**, 1 (1993).
[6] M. S. Pettersen and W. Saam, J. Low Temp. Phys. **90**, 159 (1993).
[7] K. S. Ketola and R. B. Hallock, Phys. Rev. Lett. **71**, 3295 (1993); K. S. Ketola, T. A. Moreau, and R. B. Hallock, J. Low Temp. Phys. **101**, 343 (1995).
[8] D. Ross, J. E. Rutledge, and P. Taborek, Phys. Rev. Lett. **76**, 2350 (1996).
[9] D. Ross, J. E. Rutledge, and P. Taborek, Phys. Rev. Lett. **74**, 4483 (1995).
[10] B. Clements, E. Krotscheck, and M. Saarela, Phys. Rev. B **55**, 5959 (1997).
[11] J. Klier and A. F. G. Wyatt, J. Low Temp. Phys. **116**, 61 (1999).
[12] F. Dalfovo, Z. Phys. D **14**, 263 (1989).
[13] M. Barranco *et al.*, Phys. Rev. B **56**, 8997 (1997).
[14] M. Pi, R. Mayol, and M. Barranco, Phys. Rev. Lett. **82**, 3093 (1999).
[15] F. Ancilotto, A. M. Sartori, and F. Toigo, Phys. Rev. B **58**, 5085 (1998).
[16] F. Dalfovo *et al.*, Phys. Rev. B **52**, 1193 (1995).
[17] R. Mayol *et al.*, Phys. Rev. Lett. **87**, 145301 (2001).
[18] E. Krotscheck, Phys. Rev. B **32**, 5713 (1985).
[19] J. Treiner and L. Pricaupenko, J. Low Temp. Phys. **101**, 349 (1995).
[20] S. Stringari and J. Treiner, J. Chem. Phys. **87**, 5021 (1987).
[21] E. S. Hernández, Phys. Rev. Lett. **89**, 185301 (2002).